

SPECIAL ISSUE ARTICLE

Genome-wide association mapping identifies *HvNIP2;2/HvLsi6* accounting for efficient boron transport in barley

Zhongtao Jia¹  | Manuela Désirée Bienert^{2,3}  | Nicolaus von Wirén¹  |
Gerd Patrick Bienert^{2,3} 

¹Department of Physiology and Cell Biology, Molecular Plant Nutrition, Leibniz Institute of Plant Genetics and Crop Plant Research (IPK), Gatersleben, Germany

²Department of Physiology and Cell Biology, Metalloid Transport, Leibniz Institute of Plant Genetics and Crop Plant Research (IPK), Gatersleben, Germany

³Crop Physiology, Department of Molecular Life Sciences, TUM School of Life Sciences, Technical University of Munich, Freising, Germany

Correspondence

Zhongtao Jia, Department of Physiology and Cell Biology, Molecular Plant Nutrition, Leibniz Institute of Plant Genetics and Crop Plant Research (IPK), Corrensstrasse 3, 06466 Gatersleben, Germany.
Email: zhongtao@ipk-gatersleben.de

Gerd Patrick Bienert, Crop Physiology, Department of Molecular Life Sciences, TUM School of Life Sciences, Technical University of Munich, Alte Akademie 12, 85354 Freising, Germany.
Email: patrick.bienert@tum.de

Funding information

Bundesministerium für Bildung und Forschung, Grant/Award Number: FKZ0315969D; Chinese Scholarship Council, Grant/Award Number: 201406350062; Deutsche Forschungsgemeinschaft, Grant/Award Numbers: 1668/1-1, 1668/4-1

Edited by: H. Sonah

Abstract

Boron (B) is an essential mineral element for plant growth, and the seed B pool of crops can be crucial when seedlings need to establish on low-B soils. To date, it is poorly understood how B accumulation in grain crops is genetically controlled. Here, we assessed the genotypic variation of the B concentration in grains of a spring barley (*Hordeum vulgare* L.) association panel that represents broad genetic diversity. We found a large genetic variation of the grain B concentration and detected in total 23 quantitative trait loci (QTLs) using genome-wide association mapping. *HvNIP2;2/HvLsi6*, encoding a potential B-transporting membrane protein, mapped closely to a major-effect QTL accounting for the largest proportion of grain B variation. Based on transport studies using heterologous expression systems and gene expression analysis, we demonstrate that *HvNIP2;2/HvLsi6* represents a functional B channel and that expression variation in its transcript level associates with root and shoot B concentrations as well as with root dry mass formation under B-deficient conditions.

1 | INTRODUCTION

In vascular plants, boron (B) represents an essential trace element for proper growth and development (Lewis, 2019; Wimmer et al., 2020). In addition to its unique role in cell wall maintenance, B is also

essential for human and animal nutrition because it can compensate, to some extent, for calcium in bone stability and thus strengthen the skeletal structure (Meacham et al., 1995; Nielsen et al., 1987). Boron plays important roles in plant metabolism and phytohormone homeostasis and is required for cell wall and membrane integrity (Eggert &

This is an open access article under the terms of the Creative Commons Attribution License, which permits use, distribution and reproduction in any medium, provided the original work is properly cited.

© 2021 The Authors. Physiologia Plantarum published by John Wiley & Sons Ltd on behalf of Scandinavian Plant Physiology Society.

von Wirén, 2017; Matoh, 1997; Pommerrenig et al., 2019). For example, in the pectin fraction of the primary cell wall, B functions in cross-linking two rhamnogalacturonan-II monomers in the form of borate esters (O'Neill et al., 2001), entailing that the B requirement of plants is positively correlated with the pectin content of their cell walls (Matoh et al., 1993). Optimal B supply depends on the plant species and lies in an extremely narrow range between deficiency and toxicity. Both B deficiency and B toxicity cause detrimental yield losses in agricultural and horticultural crops worldwide (Brdar-Jokanovic, 2020; Miwa et al., 2007; Shorrocks, 1997). Boron deficiency negatively impacts seedling development (Eggert & von Wirén, 2016) as well as vegetative and reproductive growth of mature plants, thus causing cessation of root and shoot elongation, reducing leaf expansion, modifying leaves (brittle), and reducing fertility (Brdar-Jokanovic, 2020; Dell & Huang, 1997). Likewise, B toxicity symptoms are manifested by chlorosis and necrosis at the tips of older leaves and by inhibition of root growth and function (Schnurbusch et al., 2010; Sutton et al., 2007).

Boron is predominantly taken up by plant roots as uncharged boric acid molecules and to a much lower extent as borate anions (Takano et al., 2008). Members of major intrinsic proteins (MIPs) and BOR transporters were shown to mediate B uptake into roots, its root-to-shoot translocation and redistribution in the shoot (Bienert & Bienert, 2017; Pommerrenig et al., 2015; Reid, 2014; Takano et al., 2008). In *Arabidopsis*, *AtNIP5;1*, a member of the nodulin 26-like intrinsic protein (NIP) family, which is a plant subgroup of the MIP family, functions as a channel protein that imports boric acid to the epidermal, cortical, and endodermal cells of roots (Takano et al., 2006). Following the uptake of B by *AtNIP5;1*, *AtBOR1*, an orthologue of bicarbonate transporters in animal cells, functions as a borate exporter involved in xylem loading of B, thus regulating the root-to-shoot translocation of B (Takano et al., 2002). In *Arabidopsis*, *AtNIP5;1* and *AtBOR1* constitute a cooperative and efficient transcellular B uptake pathway, especially under B-limiting conditions (Takano et al., 2010). Upon arrival to the shoot, *AtNIP6;1* and *AtNIP7;1*, other members of the NIP subfamily, are essential for the redistribution of B to growing shoots and floral tissues, respectively (Li et al., 2011; Tanaka et al., 2008). Moreover, *AtNIP4;1* and *AtNIP4;2*, which are specifically expressed in pollen and permeable to B, have been suggested to be crucial for pollination (Di Giorgio et al., 2016). Despite showing differential expression patterns, homologous genes of *AtNIP5;1* and *AtBOR1* were identified in many plant species including barley, maize, rice, and oilseed rape showing conserved and physiologically relevant functions in B uptake and translocation (Chatterjee et al., 2014; Diehn et al., 2019; Durbak et al., 2014; Hanaoka et al., 2014; Leonard et al., 2014; Nakagawa et al., 2007; Schnurbusch et al., 2010; Shao et al., 2018; Sutton et al., 2007; Zhang et al., 2017). For instance, *OsNIP3;1*, a close homolog of *AtNIP5;1*, is responsible for B uptake into the root, its translocation to the shoot and redistribution to developing tissues in rice (Hanaoka et al., 2014; Shao et al., 2018). In addition to NIPs and BORs, it was recently shown that members of other MIP

subfamilies, the X-intrinsic proteins (XIPs), and the tonoplast intrinsic proteins (TIPs) may also contribute to the B homeostasis in plants (Bienert et al., 2011; Bienert et al., 2019; Pang et al., 2010). There is scarce evidence suggesting that members of the plasma membrane intrinsic protein (PIP) subfamily of MIPs also may facilitate transmembrane B transport when expressed in heterologous expression systems (Dordas et al., 2000; Fitzpatrick & Reid, 2009; Kumar et al., 2014). However, the exact roles of their participation in B transport require further in planta characterization.

Gramineous crops, including barley, are relatively insensitive to B-deficient growth conditions. At the vegetative stage, the growth of barley is scarcely inhibited by B limitations. In contrast, the flowering of barley is highly sensitive to B deficiency. Boron limitation during the reproductive development of barley results in a substantial yield loss due to male sterility (Wongmo et al., 2004). Germination and seedling establishment represent further developmental phases during which crops are highly prone to B deficiency-induced growth retardation. Seeds enriched with B in the seed coat can promote seedling vigor and early-stage plant establishment, thereby having a direct impact on crop yield (Eggert & von Wirén, 2016). Seed priming with a B-containing solution greatly improves seedling vigor, seedling stress tolerance and yield in rice and wheat, and seed B concentration in rapeseed closely associates with germination success (Alamri et al., 2018; Atique-ur-Rehman et al., 2012; Eggert & von Wirén, 2013, 2016; Iqbal et al., 2017). Despite the importance of seed B pools for seedling establishment and stress tolerance, the underlying mechanisms contributing to an efficient allocation of B to the grains of barley are largely unknown.

Natural variation is a powerful resource for dissecting the genetic architecture of complex traits and for identifying and characterizing the molecular functions of genes (Jia et al., 2020; Jia, Giehl, et al., 2019; Kuhlmann et al., 2020; Schnurbusch et al., 2010; Sutton et al., 2007). Linkage or QTL mapping has provided valuable information about the genes controlling the genetic variation of B accumulation in plant tissues and/or plant responses to B toxicity (Hua et al., 2016; Liu et al., 2009; Ochiai et al., 2008; Schnurbusch et al., 2010; Sutton et al., 2007; Zhang et al., 2014). In barley, *HvBOT1* and *HvNIP2;1* were identified by integrating natural variation and linkage mapping, and subsequently cloned and characterized as functional B transporting proteins in vegetative plant tissues (Schnurbusch et al., 2010; Sutton et al., 2007). Focusing on the lack of information on B accumulation in barley grains, we first assessed the natural variation of grain B concentrations in a diverse spring barley collection and then performed genome-wide association (GWA) mapping for this trait. This approach allowed us to identify 23 QTLs underlying grain B concentration. Performing *in silico* proteoform sequence analysis, transport assays in heterologous expression systems, and B-dependent as well as tissue-specific gene expression quantifications, we show here that the gene *HvNIP2;2/HvLsi6*, underlying a major-effect QTL, contributes to B transport regulation and associates with grain B concentration.

2 | MATERIALS AND METHODS

2.1 | Plant germplasm and genotyping

The plant germplasm used in the present study consists of 221 spring barley (*Hordeum vulgare* L.) genotypes selected from the Barley Core Collection (BCC) and the barley gene bank collection maintained at the IPK Gatersleben, Germany (Table S1). The panel was propagated by single seed descent, genotyped with a 9 K iSelect chip consisting of 7864 SNPs (Comadran et al., 2012) and successfully used for genome-wide association scans for agronomic traits, salt tolerance, and root system architectural traits (Abdel-Ghani et al. 2019; Alqudah et al., 2014, 2016, 2018; Haseneyer et al., 2010; Jia, Liu, et al., 2019; Long et al., 2013; Neumann et al., 2017; Pasam et al., 2012). The whole collection consists of 126 two-rowed and 95 six-rowed accessions originating from Europe ($n = 106$), West Asia and North Africa ($n = 45$), East Asia ($n = 39$), and America ($n = 30$).

2.2 | Plant culture and sampling

The field trials were conducted in 2012 and 2014 at the IPK Gatersleben, Germany. The mapping panel was grown in a lattice square design with four replicas per accession randomly distributed in the field. Due to limited seed availability, only a part of the mapping population comprising of 138 accessions was grown in the field trial of 2014. Plots consisted of two rows of 35 seeds with a row length of 2.5 and 0.5 m between row plots. The field and disease management were in accordance with the local management practice. At maturity, the spikes were randomly collected from plants in the middle of each plot for grain B concentration determination.

For hydroponic culture, 11 barley accessions: BCC129, BCC192, BCC434, BCC436, BCC502, BCC716, BCC761, BCC1390, BCC1410, BCC1428, and BCC1541 were germinated on wet filter paper for 5 days at 4°C in the dark to synchronize germination. After that, germinated seeds were transferred to half-strength nutrient solution without Fe supply for 7 days in a growth chamber under short-day conditions in a 20°C/18°C and 10 h/14 h light-dark regime and at a light intensity of 250 $\mu\text{mol m}^{-2} \text{sec}^{-1}$ at 70% humidity. Seedlings of similar size were transferred to full nutrient solution under long-day condition with a 20°C/18°C and 16 h/8 h light-dark regime. The nutrient solution was made of ultrapure B-free MilliQ water (Merck) that has been additionally washed prior to its usage with 3 g L⁻¹ B-complexing agent Amberlite IRA-743 (Sigma) overnight to efficiently remove all traces of B from the water. Moreover, the nutrient solution itself was treated with the B-complexing agent Amberlite IRA-743 (Sigma) overnight just before its usage. The nutrient solution contained 2 mM Ca (NO₃)₂, 0.5 mM K₂SO₄, 0.5 mM MgSO₄, 0.1 mM KH₂PO₄, 0.1 mM KCl, 0.5 μM MnSO₄, 0.5 μM ZnSO₄, 0.2 μM CuSO₄, 0.01 μM (NH₄)₆Mo₇O₂₄, and 0.1 mM Fe-EDTA, either supplied with or without 1 μM H₃BO₃. The nutrient solution was renewed every 7 days. After 14 days, shoots and roots of plants cultivated under B-

sufficient (1 μM H₃BO₃) or B-deficient growth conditions (0 μM H₃BO₃) were separately harvested for the measurement of biomass, tissue B concentration, and gene expression analysis.

The barley cultivar *Morex* was hydroponically cultured as described above to investigate the B-dependent transcript regulation of *HvNIP2;2/HvLsi6* and *HvNIP2;3*. Two days after transfer to full nutrient solution, plants were exposed to B limitation by omitting boric acid from the nutrient solution. Roots and shoots were sampled before B limitation (time point 0) and at 6, 12, 24, 48, and 72 h after treatment. After 72 h of growth under B limitation, 1 μM H₃BO₃ was supplied to the hydroponic solution to investigate the effect of B resupply on the gene expression levels of *HvNIP2;2/HvLsi6* and *HvNIP2;3*. Samples were taken at 6, 12, 24, 48 h after B resupply. At the reproductive stage, different organs of soil-grown *Morex* plants were sampled: roots, flag leaf blade and sheath, rachis, and nodes I, III, and V, internode II, developing grains at Waddington (W10, non-filled grain) and milk stage (filled-grain). All samples were immediately frozen in liquid nitrogen and stored at -80°C for RNA extraction.

2.3 | Boron concentration measurements

For determining grain B concentrations of the barley accessions from the GWAS panel, seeds from the central part of at least 5 spikes were pooled and then washed three times with ultrapure water and dried at 65°C till constant weight. Approximately 250 mg of plant material was weighed and used for determining B concentrations using an inductively coupled plasma optical emission spectrometry (ICP-OES, iCAP 6000, Thermo Fisher Scientific). For the root and shoot samples from the hydroponic experiment, roots and shoots were excised at harvest, dried at 65°C, and then weighed. The dried samples were milled and approximately 50 mg of the different tissues were subjected to B measurements using a high-resolution inductively coupled plasma mass spectrometry (HR-ICP-MS, Element 2, Thermo Fisher Scientific). B concentrations of tissue samples deriving from plants grown under B-limiting conditions were below or close to the detection limit and thus not taken into account for comparative analysis.

2.4 | Statistical analysis for phenotypic traits

Restricted maximum likelihood (REML) method was applied to calculate best linear unbiased estimates (BLUEs) of B concentrations for each genotype in 2012 and 2014. In the model, genotypes and replicates were fitted as fixed and random effects, respectively. Furthermore, BLUEs of grain B concentration for a total of 135 barley accessions across 2012 and 2014 were also calculated using the REML method by fitting a mixed linear model considering genotypes as fixed and year as random effects. Repeatability (H^2) was estimated as $H^2 = \sigma_g^2 / (\sigma_g^2 + \sigma_e^2/n)$, where σ_g^2 is the genotypic variance component, σ_e^2 is the residual variance component, and n is replicates. Pairwise comparisons were carried out using Welch's *t*-test or

ANOVA. All statistical analyzes were performed in R (R Core Team, 2013).

2.5 | Genome-wide association study and candidate gene identification

BLUEs of grain B concentration were used as the phenotypic response for GWAS using the software TASSEL v.2.1 (Bradbury et al., 2007). For the marker quality control, we applied a minor allele frequency (MAF) of <5% and missing data >10%, finally leaving 6339, 6059, and 6056 informative markers for the datasets B-2012, B-2014, and B-BLUE. We performed association analysis with two mixed linear models (MLM) incorporating kinship together with principle components or kinship alone for correcting the population structure. After evaluating the inflation of *P*-values using the quantile-quantile (Q-Q) plots and the GWAS results, we found that both mixed linear models yielded similar results. Therefore, we finally presented marker-trait associations resulting from the MLM with kinship. The model used is described as: $y = X\alpha + K\mu + e$, where y is a vector of grain B concentration; α is a vector of fixed effect for the marker to be estimated; K is the kinship matrix; μ is the vector of random effect for co-ancestry, and e is the vector of residuals. The suggestive significant threshold at $-\log_{10}(P\text{-value}) > 3$ was set to claim significant marker-trait associations. Using the chromosomal LD (Jia, Liu, et al., 2019), peaks within a short distance (~ 3.5 cM) were assigned to the same QTL. The QTLs detected in 2012 and 2014 or using the B-BLUEs were considered as stable QTLs. The other QTLs were considered as year-specific QTLs.

In order to identify putative candidate genes underlying the QTLs, a systematic BLAST search against the barley genome database (<http://webblast.ipk-gatersleben.de/barley>) was performed using known genes having an impact on B nutrition, in particular B transporter genes as reported in Arabidopsis, maize, rice, or barley. Their genetic positions were localized using the POPSEQ map (Mascher et al., 2013). Taking the chromosomal linkage disequilibrium decay of ~ 3.5 cM into account (Jia, Liu, et al., 2019), genes that were spatially near to the association peak were considered as candidate genes.

2.6 | Cloning of expression constructs and barley accession-specific *HvNIP2;2/Lsi6* and *HvNIP2;3* sequences

AtNIP5;1 cDNA was optimized for expression in oocytes by adapting the codon usage (performed by GenScript®; sequence displayed in Table S2). Primers matching the *NIP* sequences were used to PCR amplify the *NIP* cDNA sequences and to generate the respective expression constructs (listed in Table S2). Primers *yHvNIP2;2_fw*, *yHvNIP2;2_rv*, *yHvNIP2;3_fw*, and *yHvNIP2;3_rv* (Table S2) were used to PCR-clone both *NIP* genes from cDNAs of

the different natural barley accessions. The primer pair designed to amplify *HvNIP2;2* did also amplify *HvNIP2;3* and vice versa. Therefore, the resulting PCR products (containing both *HvNIP2;2* and *HvNIP2;3*) of two independent PCR reactions per barley accession were cloned into pYeDP60u and up to 85 individual pYeDP60u: *HvNIP2;x* constructs per barley accession (confirmed by a selective restriction digest) were sent for sequencing (EUROFINS) to ensure that CDSs of *HvNIP2;2* and *HvNIP2;3* were present. Based on the sequencing results, full-length CDSs of *HvNIP2;2* and *HvNIP2;3* were obtained for most of the barley accessions. For the two accessions BCC1428 and BCC129, only *HvNIP2;2* but not *HvNIP2;3* was obtained (Figure S3).

To generate *NIP* expression constructs, PCR products were cloned into the USER-compatible *Xenopus laevis* expression vector pNB1u and/or the *Saccharomyces cerevisiae* expression vector pYeDP60u using an uracil excision-based improved high-throughput USER cloning technique (Nour-Eldin et al., 2006). All sequences were verified by sequencing (Eurofins Genomics).

2.7 | Transport assays in yeast and *X. laevis* oocytes

The *S. cerevisiae* yeast strain $\Delta atr1/YML116w/Y06516/BY4741$ (EUROSCARF) was transformed with either the empty vector pYeDP60u (negative control) or pYeDP60u expressing the indicated *NIP* cDNAs. Transformed $\Delta atr1$ yeast mutant cells were selected on synthetic medium containing 2% glucose, 50 mM succinic acid/Tris base, pH 5.5, 1% yeast nitrogen base without amino acids (Difco), and 2% agar. For the boric acid and germanium dioxide toxicity growth assays, 2% galactose, 50 mM succinic acid/Tris base, pH 5.5, 1% yeast nitrogen base without amino acids (Difco), and different concentrations of boric acid or germanium dioxide were used for the growth media. Cultures of $\Delta atr1$ mutant yeast cells were diluted in sterile water and spotted on medium containing the indicated concentrations of boric acid or germanium dioxide. Growth was documented at 8 days after incubation at 30°C. The toxicity growth assay was repeated twice with similar results.

For the boric acid uptake assay, oocytes were injected with 50 nL *NIP* cRNAs (12.5 ng *NIP* cRNA per oocyte) of *HvNIP2;2/HvLsi6*, *HvNIP2;3*, *AtNIP5;1* or equal volume of RNase-free water as a negative control. The oocyte isolation and selection as well as the in vitro cRNA synthesis using the generated *NIP*-containing pNB1u vectors were performed as described by Pommerrenig et al. (2020). Three days after the cRNA injection, oocytes (7–14 oocytes per replicate; 3–10 replicates) were incubated for 20 min in Barth buffer (pH 7.4) containing 5 mM ^{10}B boric acid (Sigma-Aldrich). Afterwards, the oocytes were swiftly washed three times in Barth buffer with 5 mM ^{11}B boric acid (Sigma Aldrich) and dried for B quantification by high-resolution ICP-MS analysis. Uptake assays were repeated with oocytes isolated from two to three different *Xenopus* and were showing consistent results.

2.8 | Reverse transcription quantitative polymerase chain reaction (RT-qPCR)

Plant tissues were collected by excision and immediately frozen in liquid N. Total RNA was extracted with RNeasy Plant Mini Kit (Macherey-Nagel GmbH & Co KG). cDNA was synthesized out of 1000 ng total RNA using MuLV-Reverse Transcriptase (Fermentas) in a total volume of 20 μ l and diluted to 1:20 with nuclease-free water. RT-qPCR was performed in a 384 well thermocycler (CFX384 Touch TM Real-Time PCR Detection System, Bio-Rad) using the GoTaq qPCR Master mix (Promega). 2 μ l diluted cDNA (1:20) was used per reaction. Three identically treated biological replicates were run. The thermocycler protocol was as follows: 3 min at 95°C, followed by 45 cycles of 10 s at 95°C, and 40s at 60°C. The specificity of the primers (Table S2) was validated by BLASTN analysis and sequencing of obtained qPCR products. For the generation of a standard curve, a pool of all samples was combined into a mixture. This mixture was serially diluted (1 to 1, 1 to 2, 1 to 4, 1 to 8, 1 to 16, 1 to 32, and 1 to 64) with nuclease-free water to generate standard curve templates and to determine PCR efficiencies for each primer pair. Only assays producing PCR efficiencies >90% and < 115% were used for expression data analyzes. Cq-values of each sample and target were converted to quantities using the standard curves. Relative expression of all genes was normalized to the geometric mean of *HvADP* and *HvUBC* as internal references.

3 | RESULTS

3.1 | Phenotypic variation of the grain B concentration

Boron concentrations were determined in the grains of 218 and 138 spring barley accessions grown in field trials in 2012 and 2014, respectively. The phenotypic values of grain B concentration of individual genotypes in each year and a subpanel across 2 years followed approximately normal distribution (Figure 1), suggesting that the B concentration in the grain is a polygenic trait. A distinct genotypic variation was observed for B concentration, ranging from 0.13 μ g·g⁻¹ to 2.53 μ g·g⁻¹ and 0.55 μ g·g⁻¹ to 1.44 μ g·g⁻¹ in the respective year and from 0.55 μ g·g⁻¹ to 1.50 μ g·g⁻¹ across 2 years in a subpanel containing 135 common accessions (Table S1). Analysis of variance (ANOVA) revealed a significant genotypic effect for grain B concentrations ($P < 0.01$). In accordance, the repeatability values (H^2) were 0.58 and 0.83 in 2012 and 2014, respectively.

3.2 | Genome-wide association scans for grain B concentrations

In order to dissect the genetic architecture of the grain B concentration, we performed genome-wide association (GWA) analyzes using the grain B concentration datasets in 2012 and 2014 as well as genetic means

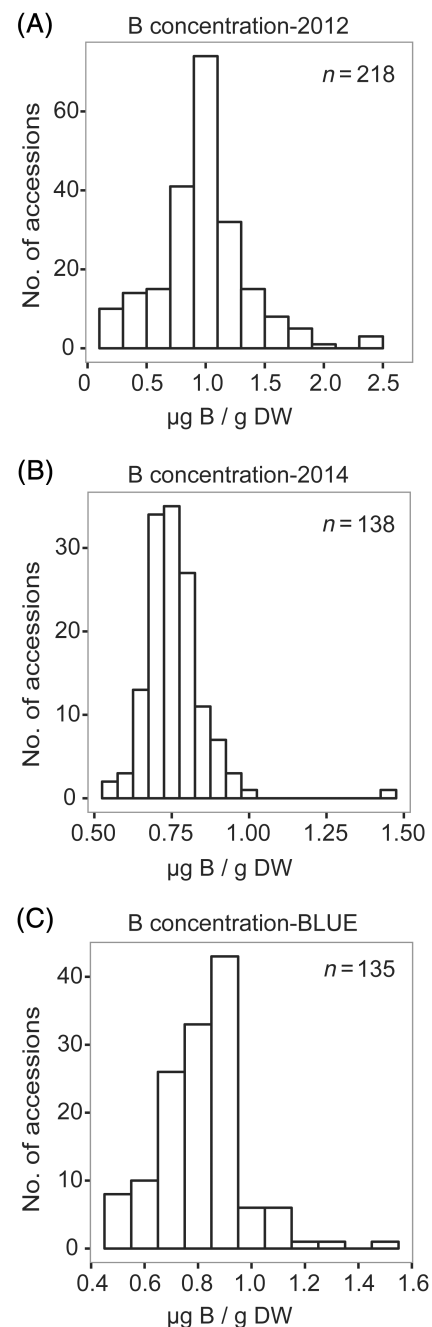


FIGURE 1 Phenotypic variation of grain boron (B) concentrations of field-grown barley accessions. Grain B concentration (μ g B/g DW) of 218, 138, and 135 spring barley accessions grown in (A) 2012, (B) 2014, and (C) BLUE (best linear unbiased estimates of B concentrations for each genotype in the year 2012 and 2014)

(BLUEs) across 2 years of a common subpanel containing 135 lines. We detected a total of 51 marker-trait associations comprised of 18, 16, and 17 significant SNPs for the respective dataset (Figure 2A–C, Table S3). These marker-trait associations are distributed over all seven chromosomes (Chrs), with numbers varying from 3 on Chr 6H to 10 on Chr 2H and 3H (Figure 2A–C, Table S3). Fourteen of these 51 significantly associated SNPs explained more than 10% of the phenotypic variation of the

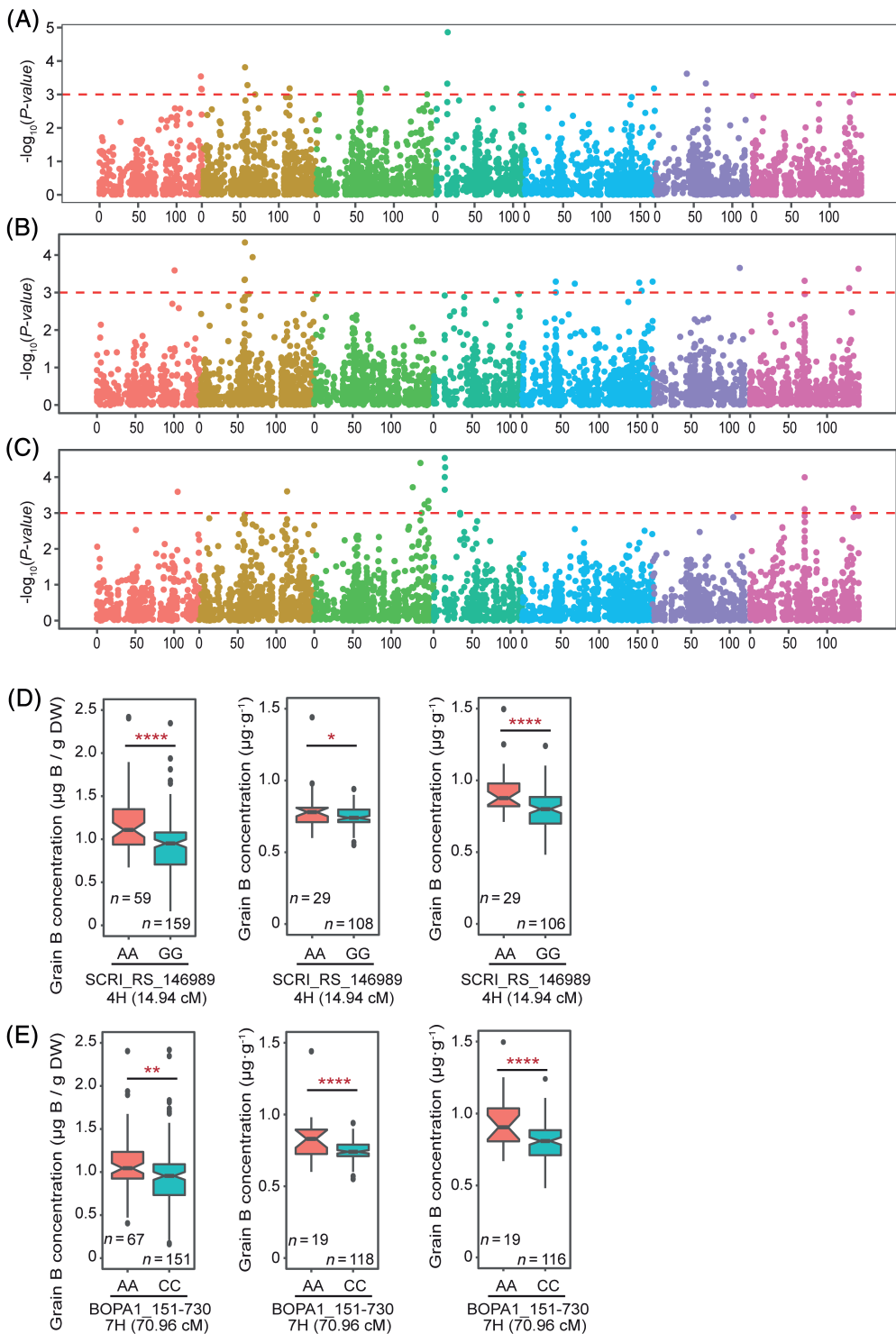


FIGURE 2 Genome-wide association scans for grain boron (B) concentration in a spring barley panel. Manhattan plots of association analyzes for grain B concentration of a spring barley panel in (A) 2012, (B) 2014, and (C) BLUE (best linear unbiased estimates of B concentrations for each genotype in the year 2012 and 2014). The seven chromosomes are distinguished by different colors. The red-dashed horizontal lines correspond to a significance threshold at $-\log_{10}(P\text{-value}) > 3$. (D, E) Boxplots showing allele effects of SNP marker (D) SCRI_RS_146989 and (E) BOPA1_151-730 on grain B concentrations ($\mu\text{g B/g DW}$) in 2012 (left panel), 2014 (middle panel), and across 2 years (right panel). Asterisks indicate statistically significant differences between two alleles according to an ANOVA test. Values below each boxplot in (D) and (E) indicate the number of accession (*n*) carrying the alternative allelic variant for the associated SNP ($P < 0.05$, $**P < 0.01$, $****P < 0.0001$)

grain B concentration (Table S3). Using the chromosomal linkage disequilibrium (LD) decay of the panel (Jia, Liu, et al., 2019), the 51 significant SNPs were assigned into 23 genetically linked QTL intervals (Table S4). Among them, 11 QTLs were either detected using BLUEs across 2 years or consistently detected in both cultivation years, 2012 and 2014 (Table S4), thus considered as stable QTLs. In addition, there were 7- and 5-year-specific QTLs for 2012 and 2014, respectively (Table S4). The most significant-associated QTL, rated according to the $-\log_{10} P\text{-value}$ calculation, was detected on Chr 4H (qB11, 14.43–14.94 cM), with the most

significantly associated marker SCRI_RS_146989 explaining 11.04% of the natural variation of the grain B concentration. The accessions carrying the minor allele “A” at this locus on average had 31.4, 5.5, and 17.3% significantly higher B concentrations than those expressing the “G” allele in 2012, 2014, and across the 2 years (Figure 2D). Another genomic region with three markers was identified on Chr 7H (qB21, 70.61–70.96 cM). At this locus, analysis of the SNP effect showed that genotypes expressing the minor allele “A” had 15.8, 13.1, and 18.8% higher B concentrations than those with the “C” allele (Figure 2E).

3.3 | Identification of candidate genes underlying the QTLs associated with the grain B concentration

To explore the putative candidate genes underlying the detected QTLs, we made a homology search of genes having an impact on B nutrition, in particular B transporters or channels, against the IPK Barley Genome Database (<http://webblast.ipk-gatersleben.de/barley>) and identified a number of high-priority candidates (Table S3). We found that *HvBOR1* (Chr 5H, 42.98 cM, morex_contig_47944), orthologous to *OsBOR1* (Nakagawa et al., 2007), was closely linked to *qB14* (Chr 5H, 43.76 cM). *HvPIP1;4* (Chr 6H, 59.91 cM, morex_contig_280723) and *HvPIP1;3* (Chr 6H, 118.98 cM, morex_contig_1569089) mediating B transport in yeast cells (Fitzpatrick & Reid, 2009) mapped close to *qB19* (Chr 6H, 65.93 cM) and *qB20* (Chr 6H, 113.24 cM), respectively. *HvPIP2;5* was a likely candidate for *qB3*, *HvPIP2;3* and *HvPIP2;4* for *qB4*, *HvTIP4;2* and *HvTIP4;3* for *qB6*, *HvPIP2;11* and *HvTIP4;1* for *qB13*, *HvPIP2;8* and *HvPIP2;12* for *qB17*. Furthermore, *qB21* (Chr 7H, 70.61–70.96 cM) mapped closely to a previously functionally characterized and physiologically important Si transporter *HvNIP2;2/HvLsi6* (Chr 7H, 61.02 cM, morex_contig_1633799) and a non-characterized NIP gene *HvNIP2;3* (Chr 7H, 67.63 cM, morex_contig_45067). In the

barley cv. *Morex* genome, both genes are located approximately 467 kb from each other and are only separated by four putative pseudogenes (Figure S1). The *HvNIP2;2/HvLsi6* and *HvNIP2;3* coding and protein sequences have an identity of 96.5% and 97.3%, respectively, suggesting similar functionality.

3.4 | Candidate genes *HvNIP2;2/HvLsi6* and *HvNIP2;3* transport boric acid in yeast and *X. laevis* oocytes

Heterologous expression assays in the yeast *S. cerevisiae* and *X. laevis* oocytes were used to assess the potential B transport activity of the channel proteins encoded by the two candidate genes *HvNIP2;2/HvLsi6* and *HvNIP2;3* identified in *qB21*, in which the significantly associated SNP accounted for the largest proportion of phenotypic variation ($R^2 = 16.92\%$). The *S. cerevisiae* mutant strain $\Delta atr1$ is highly sensitive to high B conditions because it lacks the endogenous B efflux transporter *ATR1* involved in B detoxification. This strain is, therefore, suitable for a growth suppression assay to functionally assess transporter proteins permeable to boric acid. We found that the expression of the positive

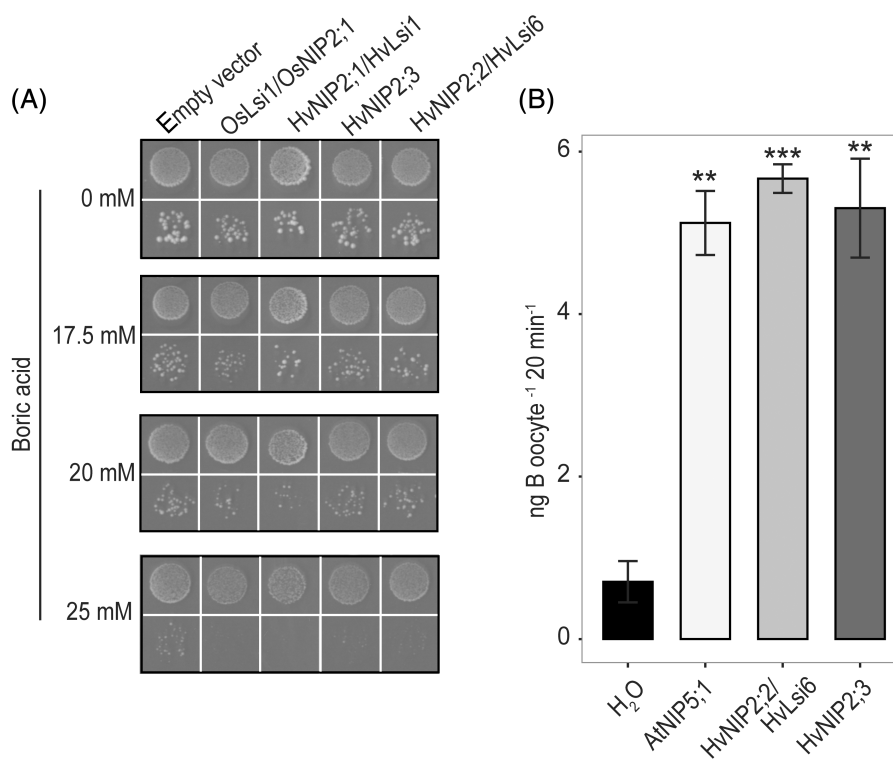


FIGURE 3 Boric acid transport activity of *HvNIP2;2/HvLsi6* and *HvNIP2;3* in yeast and *Xenopus laevis* oocytes. (A) Boron toxicity growth assay on increasing B concentrations in the growth media using the $\Delta atr1$ mutant yeast strain expressing the indicated NIP isoforms or the empty vector control. The empty vector was used as a negative control, whereas *OsLsi1/OsNIP2;1* and *HvNIP2;1/HvLsi1* were used as positive controls. Growth behavior and survival rates of different transformants were recorded after 8 days at 30°C and were shown for yeasts spotted at an OD_{600} of 0.01 (upper row) and 0.0001 (bottom row). (B) Transport activity of indicated NIP proteins for boric acid in *X. laevis* oocytes. cRNA of *AtNIP5;1* as a positive control, *HvNIP2;2/HvLsi6*, *HvNIP2;3*, or water as a negative control were injected into *X. laevis* oocytes. B levels were quantified by ICP-MS technology. Bars represent mean \pm SE of two to three independent experiments (each having 3–10 replicates with 7–14 oocytes per replicate). Asterisks indicate statistically significant differences between oocytes injected with cRNAs of NIPs and water (negative control) according to Welch's *t*-test (** $P < 0.01$, *** $P < 0.001$)

controls *OsLsi1/OsNIP2;1* and *HvNIP2;1/HvLsi1*, both permeable to boric acid (Schnurbusch et al., 2010), caused growth inhibition of yeast cells under high B concentrations compared to the expression of the empty vector previously shown to be non-functional in yeast (Figure 3A). Comparable to the positive controls *OsLsi1/OsNIP2;1* and *HvNIP2;1/HvLsi1*, the expression of either *HvNIP2;2/HvLsi6* or *HvNIP2;3* inhibited the growth of yeast cells exposed to high B concentrations in the growth medium (Figure 3A). To confirm these results in an independent experimental approach, we further expressed *HvNIP2;2/HvLsi6* and *HvNIP2;3* in *X. laevis* oocytes to examine their B transport activity in a quantitative B uptake assay using isotope discrimination technology. *AtNIP5;1* is permeable to boric acid in the oocyte system (Takano et al., 2006) and was used as a positive control. Compared to oocytes injected with water, oocytes injected with cRNA of *AtNIP5;1*, *HvNIP2;2/HvLsi6* and *HvNIP2;3* showed a more than seven-fold higher B uptake activity (Figure 3B).

We further tested whether *HvNIP2;2/HvLsi6* and *HvNIP2;3* conduct silicic acid (Si) using germanic acid, a proven transport analog (Ma et al., 2006; Schnurbusch et al., 2010) toxic to yeast cells at high concentrations. Consistent with previous findings showing that *HvNIP2;2/HvLsi6* is able to transport Si (Yamaji et al., 2012), the toxicity growth assay showed that expression of either *HvNIP2;2/HvLsi6* or *HvNIP2;3* can largely suppress yeast growth compared yeast expressing the negative controls: the empty vector or *AtNIP5;1* (Figure S2). In summary, the results from these transport assays indicate that both *HvNIP2;2/HvLsi6* and *HvNIP2;3* facilitate the transport of B and Si.

3.5 | *HvNIP2;2/HvLsi6* and *HvNIP2;3* proteoform variations in natural barley accessions cannot explain their genetic association with grain B concentrations

To investigate whether protein sequence variations and subsequent proteoform-specific transport characteristics may contribute to contrasting B translocation efficiencies to the grain, 10 natural barley accessions with contrasting grain B concentrations were selected to clone and compare the *HvNIP2;2/HvLsi6* and *HvNIP2;3* sequences (Figure S3A). For most of the chosen barley accessions, both genes were cloned and sequenced in full-length. None of the cDNA-derived proteoforms could be closely associated with either a high or a low B concentration in the grains (Figure S3B). For *HvNIP2;3*, we did not identify any amino acid variation among the high- and low-B accumulating groups. For *HvNIP2;2/HvLsi6*, three out of five high-B accumulating barley accessions shared one amino acid exchange in the N-terminus of *HvNIP2;2/HvLsi6*, which was not found in low-B accumulating barley accessions. However, two other high-B accumulating accessions displayed an identical protein sequence to the one found in all low-B accumulating barley accessions. The fact that no high- or low-B accumulating barley accession was defined by only one proteoform suggested that the expression pattern or level of *HvNIP2;2/HvLsi6* and/or *HvNIP2;3* was responsible for the QTL-underlying process leading to differential grain B concentrations.

3.6 | Developmental-, tissue-, and B-dependent expression patterns of *HvNIP2;2/HvLsi6* and *HvNIP2;3* in barley

To understand the potential consequences of *HvNIP2;2/HvLsi6* and *HvNIP2;3* expression on B allocation in whole plants, we investigated the expression pattern of these two genes in different organs at different development stages. RNA-seq data from the International Barley Genome Sequencing Consortium (2012) suggested that both *HvNIP2;2/HvLsi6* and *HvNIP2;3* are expressed in diverse organs and that the transcript abundance of *HvNIP2;2/HvLsi6* is 4- to 37-fold higher than *HvNIP2;3* in all tested organs (Figure S4). At the vegetative stage, we found that *HvNIP2;2/HvLsi6* and *HvNIP2;3* were expressed in the root and the shoot. However, the transcript abundance of *HvNIP2;2/HvLsi6* and *HvNIP2;3* was 5- and 50-fold higher in shoots than in roots, respectively (Figure 4A,B,E,F). Consistent with the expression profiles obtained from RNA-sequencing (Figure S4), we found that the expression level of *HvNIP2;2/HvLsi6* was 93- and 9-fold higher than *HvNIP2;3* in roots and shoots, respectively (Figure 4A,B,E,F). We then performed a time-course analysis of *HvNIP2;2/HvLsi6* and *HvNIP2;3* transcript abundance in roots and shoots under B-limiting growth conditions and after B resupply. In roots, the expression level of *HvNIP2;2/HvLsi6* was slightly but significantly enhanced after 12 h of B deprivation, while the expression of *HvNIP2;3* was significantly upregulated only 48 h after onset of B starvation (Figure 4A,E). In contrast to roots, the shoot expression level of both genes was rapidly and significantly downregulated by B limitation (Figure 4B,F). After B resupply, the expression level of none of the genes was significantly changed, neither in roots nor in shoots (Figure 4C,D,G), except for *HvNIP2;2/HvLsi6*, which was slightly but significantly downregulated in the shoot (Figure 4D). At the reproductive stage, *HvNIP2;2/HvLsi6* and *HvNIP2;3* were expressed in nodes, the flag leaf, rachis, and developing grains in addition to roots (Figure 4I). Furthermore, in developing grains, we found that transcript abundance was approximately 105- and 43-fold higher in non-filled grains at the Waddington stage (W10) compared to those of filled grains at milk stage for *HvNIP2;2/HvLsi6* and *HvNIP2;3*, respectively (Figure 4I).

3.7 | Transcript abundance of *HvNIP2;2/HvLsi6* quantitatively contributes to efficient B uptake and B shoot translocation in natural barley accessions

To estimate whether *HvNIP2;2/HvLsi6* and/or *HvNIP2;3* expression levels contribute to efficient B transport and accumulation in barley, 11 natural barley accessions with contrasting grain B concentrations were selected and then hydroponically cultured with or without 1 μ M B supply. After 14 days, we analyzed the expression level of both genes in roots by qPCR and determined root and shoot biomass as well as their B concentrations. The B concentration and biomass of roots and shoots differed amongst accessions (Figures S5 and S6). The expression level of *HvNIP2;2/HvLsi6* and *HvNIP2;3* also differed

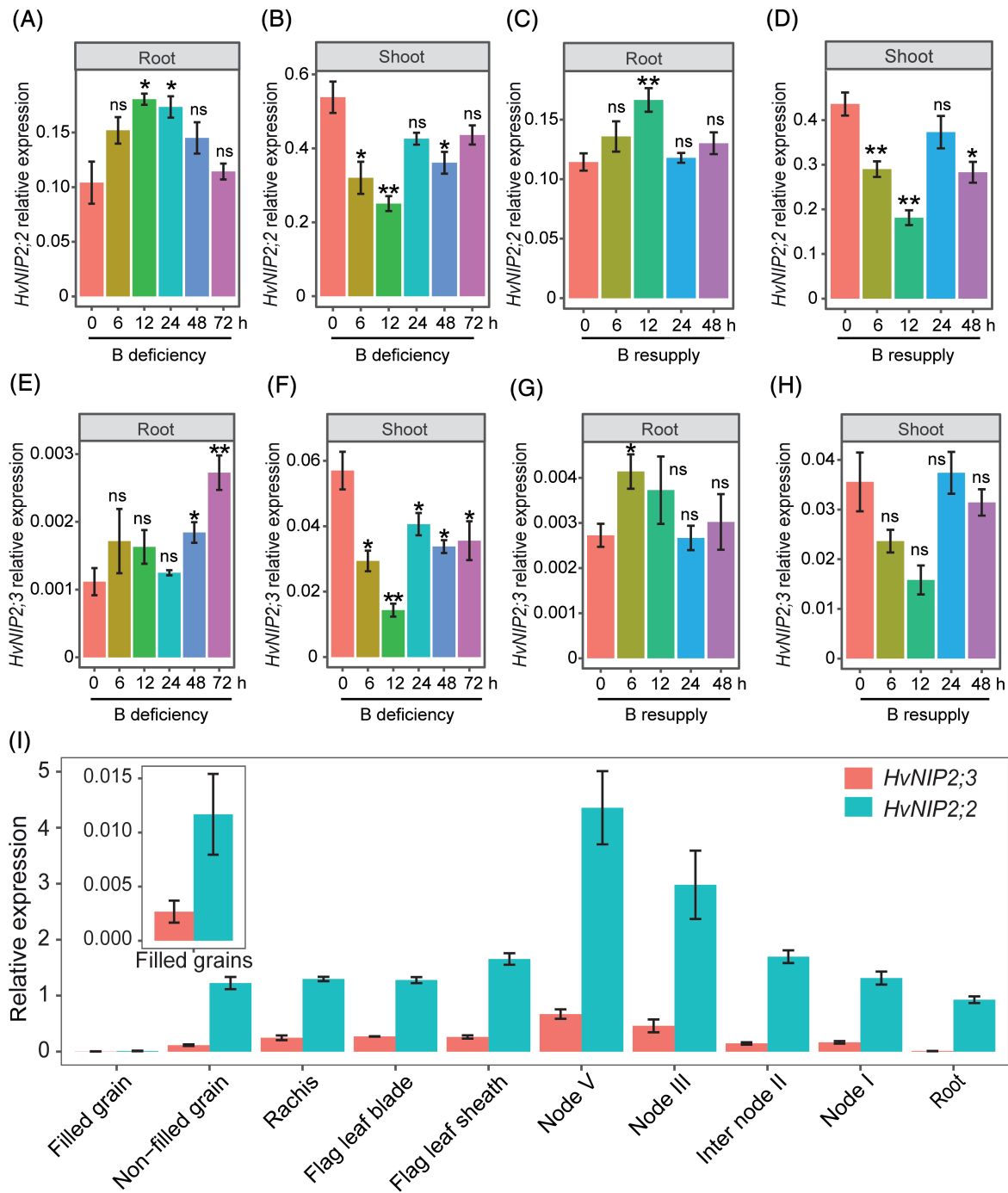


FIGURE 4 Expression patterns of *HvNIP2;2/HvLsi6* and *HvNIP2;3* in different organs at different development stages of *Morex* barley plants. Regulation of *HvNIP2;2/HvLsi6* (A,B) and *HvNIP2;3* (E,F) expression by B limitation in roots (A,E) and shoots (B,F) of 9–12-day-old plants. Relative expression of *HvNIP2;2/HvLsi6* (C,D) and *HvNIP2;3* (G,H) in roots (C,G) and shoots (D,H) in response to 1 μ M B resupply in 12–14 days old plants. (I) Expression pattern of *HvNIP2;2/HvLsi6* and *HvNIP2;3* in different organs at flowering stage. Relative expression levels were quantified by RT-qPCR. *HvADP* and *HvUBC* have been used as reference genes. Bars represent mean \pm SE of three biological replicates. Asterisks indicate statistically significant differences between the relative expression values at the respective time point and B treatment and the initial time point “0” according to Welch’s *t*-test (**P* < 0.05, ***P* < 0.01; ns, not significant)

among the accessions (Figure S7). We found that the expression level of *HvNIP2;2/HvLsi6* in roots significantly correlated with B concentrations in roots and in shoots under adequate B supply, suggesting that the variation in transcript abundance of *HvNIP2;2/HvLsi6* contributes to B uptake (Figure 5A,B). Under B deficiency, the expression level of

HvNIP2;2/HvLsi6 was significantly and positively associated with the root dry mass (Figure 5C). Furthermore, the fold-change of the relative expression level of *HvNIP2;2/HvLsi6* (B-deficient versus B-sufficient growth conditions) was also significantly associated with the relative root dry biomass between B-deficient and B-sufficient

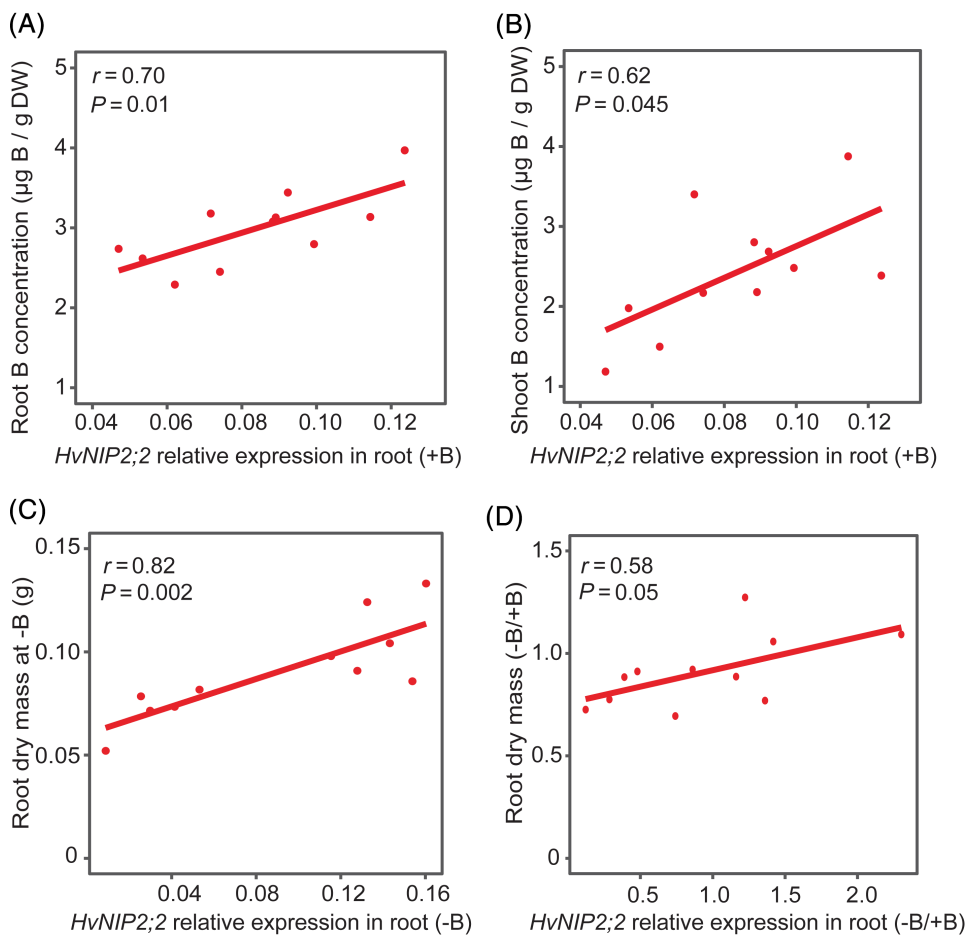


FIGURE 5 Transcript levels of *HvNIP2;2/HvLsi6* associate with the natural variation of B-dependent root and shoot dry mass production in natural barley accessions. (A, B) Pearson's correlation between the transcript level of *HvNIP2;2/HvLsi6* and the B concentration in roots (A) and shoots (B) of natural barley accessions. (C) Pearson's correlation between the transcript level of *HvNIP2;2/HvLsi6* and root biomass accumulation under B deficiency. (D) Pearson's correlation between the transcriptional alteration of *HvNIP2;2/HvLsi6* and root biomass in response to B limitation. Relative expression levels were quantified by RT-qPCR and normalized to geometric mean of *HvADP* and *HvUBC* as internal references. Each value represents the mean of three biological replicates at the respective B condition

growth conditions (Figure 5D). These results indicated that the gene expression of *HvNIP2;2/HvLsi6* under B-deficient growth conditions associates with genotypic differences in root biomass production. In contrast to *HvNIP2;2/HvLsi6*, the expression level of *HvNIP2;3* showed neither a correlation to B tissue concentrations nor to the root dry mass at any of the B treatments (Figure S8). In summary, these results suggested that the expression level of *HvNIP2;2/HvLsi6* quantitatively contributes to efficient B uptake and that *HvNIP2;2/HvLsi6* is a relevant determinant for tolerance against B deficiency.

4 | DISCUSSION

Compared to most dicot crop species, cereals require relatively little B to fulfill their life cycles (Lordkaew et al., 2011; Lordkaew et al., 2013). Early seedling establishment and the reproductive growth phase represent two developmental periods in which cereals are sensitive to B deprivation. Interestingly, the seedling growth of most barley cultivars appears to be highly insensitive to B-limiting conditions. One reason explaining this phenomenon might be the ability of barley to store sufficient amounts of B in its seeds to build a reservoir that can be remobilized and used in early growth stages until an efficient nutrient foraging root system has been developed. Aiming at dissecting genetic

factors that quantitatively determine B levels in barley grains, we investigated the natural variation of grain B accumulation and performed GWAS to identify genomic loci and underlying candidate genes. Twenty-three QTLs were found associated with grain B accumulation and a few of them co-located with potential B transporter genes. In particular, one major-effect QTL closely located to *HvNIP2;2/HvLsi6* raised interest as the corresponding gene product represents a metalloiodoporphin and is suggested to mediate the transport of B across membranes.

Natural variation is the basis for crop improvement and the identification of key genes underlying complex agronomic traits (Jia et al., 2020; Jia, Giehl, et al., 2019; Kuhlmann et al., 2020; Schnurbusch et al., 2010; Sutton et al., 2007). Like observed in other plant species, such as rice (C. C. Wang, Tang, et al., 2020; Yang et al., 2018), wheat (Jamjod et al., 2004), and *Brassica napus* (W. Wang, Ding, et al., 2020), grain B concentrations in a panel of 135 field-grown barley accession lines differed by up to threefold (Figure 1, Table S1). Grain B accumulation depends on multiple transport steps involving (1) B uptake by the root, (2) root-to-shoot translocation, (3) B allocation to various tissues, and (4) B loading into grains. Thus, B grain accumulation is expected to be a complex quantitative trait. In fact, this assumption was supported by our findings as grain B concentrations followed a normal distribution (Figure 1) and as the GWAS detected a total of 23 QTLs that were significantly associated

with grain B concentrations (Figure 2, Table S3). Fifteen of these QTLs explained less than 10% of the natural variation, suggesting that the quantity of B in barley grains is genetically controlled by many additive genetic loci with small to moderate effects contributing to the phenotypic variation. In fact, a similar finding was made in rice. In a very recent QTL study, C. C. Wang, Tang, et al. (2020) detected two QTLs associated with rice grain B concentration in a Recombinant Inbred Line (RIL) population, with each QTL explaining only about 7% of the phenotypic variation.

In accordance with the fact that several transport steps contribute to grain B accumulation, several of the identified QTLs co-located with genes from the MIP and BOR transporter families, which are known to comprise isoforms mediating physiologically relevant B fluxes in various plant species. In *Arabidopsis* and rice, AtBOR1 and OsBOR1, respectively, are expressed in the vascular cylinder and are involved in the root-to-shoot translocation of B (Nakagawa et al., 2007; Takano et al., 2002). We found that their orthologous gene, *HvBOR1*, is located in the vicinity to *qB14* on Chr 5H, and thus, represents a promising candidate gene underlying this locus. In barley, *HvBOR2/HvBOT1* and *HvNIP2;1/HvLsi1*, which were demonstrated to represent the causative genes in major QTLs associated with B toxicity (Schnurbusch et al., 2010; Sutton et al., 2007), were not closely linked to any of the identified QTLs in this study, suggesting that they may not contribute significantly to the genotypic differences in grain B levels in the investigated accession panel. An alternative explanation for their lack of identification might be that rare alleles of *HvBOR2/HvBOT1* and *HvNIP2;1/HvLsi1* contribute to the natural variation associated with barley grain B concentration. In this case, they are likely to be missed in the GWAS performed here because this approach is only able to detect common genetic variants. As such, future genetic analysis using, for instance, progenies generated from biparental populations of parental lines with contrasting seed B levels will provide a complementary view of the genetic architecture determining grain B accumulation in barley.

XIPs and TIPs have also been implicated in B transport through functional analysis either *in vivo* using transgenic plants or *in vitro* via transport assays in heterologous expression systems (Bienert et al., 2011; Bienert et al., 2019; Pang et al., 2010). When over-expressed, AtTIP5;1 increases the tolerance of transgenic *Arabidopsis* plants to high B, most likely via vacuolar compartmentation (Pang et al., 2010). We found three TIPs (*HvTIP4;2*, *HvTIP4;3* and *HvTIP4;1*) in close linkage with *qB6* and *qB13*. Moreover, we identified *HvPIP1;4* and *HvPIP1;3*, which were previously shown to facilitate the transmembrane diffusion of B in a yeast B toxicity tolerance assay (Fitzpatrick & Reid, 2009) and appeared as candidate genes underlying *qB19* and *qB20*. Whether these PIP-type aquaporins, which usually fulfill physiological functions in plant water homeostasis (Maurel et al., 2015), represent functionally relevant B transporters or whether their water transport function indirectly influences B transport processes in barley remains to be investigated. Similar to our finding that PIP genes co-localize with QTLs for grain B concentrations in barley, *PIP2A* and *PIP2;7* were identified in two QTLs determining grain B concentration in rice and have thus been suggested to

represent the underlying candidate genes (C. C. Wang, Tang, et al., 2020). It will be necessary to investigate in future studies the role in B homeostasis of the other NIP, BOR, TIP, and PIP proteins, which were located within the by us identified QTL regions.

HvNIP2;2/HvLsi6 was previously characterized as a Si transporter crucial for Si distribution in barley (Yamaji et al., 2012). We found that the major-effect QTL *qB21* coincides with this NIP gene and its nearby tandem duplicate *HvNIP2;3*. It was estimated that this QTL, encompassing both NIP metalloiodoporphin genes, contributes to 16% of the natural variation in grain B concentration, indicating that this locus may play a major role in this trait. The evolution of transport proteins duplicated in the genome, for instance in tandem, represents a likely source for sub-functionalization of the resulting proteoforms, either in terms of a selectivity shift or spatiotemporal expression differences, and thus diverging transport features or capacities between the proteoforms (Hanikenne et al., 2008). Differential evolution of these tandem-localized *HvNIP2* genes in different natural barley accessions might have created cultivars with different functional properties either due to different transport characteristics of the proteins themselves or due to different spatiotemporal expression patterns and/or levels. Thus, we chose these two NIP2-type genes for further characterization.

NIPs transport a broad range of substrates, including glycerol, ammonia, urea, water, hydrogen peroxide, and the metalloids arsenic (As), antimony (Sb) selenium, Ge, Si, and B (Bienert & Bienert, 2017). Despite this broad substrate spectrum, the physiological relevance of NIPs in planta appears restricted to the uptake and translocation of the essential and beneficial metalloids B and Si, respectively, but also to the extrusion of the toxic minerals As, Sb, and Ge (Bienert & Bienert, 2017; Pommerrenig et al., 2015). Therefore, it was plausible to hypothesize that *HvNIP2;2/HvLsi6* and *HvNIP2;3* can transport B in addition to Si, particularly as NIP2-type channels represent “non-selective” metalloiodoporphins able to facilitate the transmembrane transport of As, Si, and B equally well (Mitani-Ueno et al., 2011; Pommerrenig et al., 2015). Such a co-permeability for both B and Si was also demonstrated for *HvNIP2;1/HvLsi1* (Chiba et al., 2009; Schnurbusch et al., 2010). In fact, we found by heterologous expression in yeast that both *HvNIP2;2/HvLsi6* and *HvNIP2;3* facilitate the transport of B in addition to Si (Figure 3A and Figure S2), indicating that they are able to act as Si and B channels in planta. Further supporting evidence for their ability to transport B was obtained in quantitative B uptake assays using $^{10}\text{B}/^{11}\text{B}$ isotope discrimination. When expressed in oocytes, both proteins mediate B uptake rates similar to the well-characterized boric acid channel AtNIP5;1 essential for B nutrition in *A. thaliana* (Figure 3B). Taken together, our results define *HvNIP2;2/HvLsi6* and *HvNIP2;3* as functional B transporters. A protein sequence comparison of *HvNIP2;2/HvLsi6* and *HvNIP2;3* between natural barley accessions contrasting in their grain B concentrations did not identify *HvNIP2;2/HvLsi6* or *HvNIP2;3* proteoforms that can convincingly explain high or low grain B concentrations (Figure S3). Noteworthy, three out of five analyzed high-B accumulating barley accessions encoded for a *HvNIP2;2/HvLsi6* proteoform

with one amino acid variation in the very N-terminus of the protein at position 11 close to a putative phosphorylation site (Figure S3). Whether this variant affects B accumulation in barley will be analyzed in future studies. It might be that this mutation is sufficient but not necessary to exert an impact on B accumulation as the majority of the high and low-B accumulating accessions encoded for sequence-wise identical HvNIP2;2/HvLsi6 and HvNIP2;3 proteins (Figure S3B). To assess the B transport ability in yeast and oocytes, we functionally examined the HvNIP2;2/HvLsi6 and HvNIP2;3 proteoform variants (Figure S3B) predominately found in high- and low-B accumulating accessions. Our protein sequence comparison analysis suggested that the contribution of HvNIP2;2/HvLsi6 and/or HvNIP2;3 to contrasting grain B concentrations in barley accessions is likely related to other factors than proteoform variation.

Our comprehensive qPCR-based expression analysis proposed that *HvNIP2;2/HvLsi6* is a likely candidate gene underlying the detected *qB21* locus though we cannot exclude the additional involvement of other genes in the associated regions. On the one hand, this gene was more abundantly expressed than *HvNIP2;3* (Figure 4). On the other hand, we found that there is no significant association between the expression levels of *HvNIP2;3* and B concentration in different accessions (Figure S8), whereas the transcript level of *HvNIP2;2/HvLsi6* significantly correlated with B concentrations in roots and in shoots of natural accessions selected for contrasting grain B concentrations (Figure 5A,B). These results suggested that allelic variants of *HvNIP2;2/HvLsi6* may cause variations in transcript levels that contribute to the natural variation in B accumulation. Future resequencing of *HvNIP2;2/HvLsi6* genomic regions in the examined barley germplasm may allow for the identification of haplotypes and allelic variants that contribute to the development of molecular markers that can be used for breeding B-efficient barley lines. In roots, *HvNIP2;2/HvLsi6* is expressed in the epidermis and cortex of root tips, relevant for the uptake of the metalloids Si and B. The expression of *HvNIP2;2/HvLsi6* is not regulated by the external Si supply (Yamaji et al., 2012). Distinct from these results, we found that *HvNIP2;2/HvLsi6* expression is slightly but significantly upregulated by B deprivation (Figure 4A). Whether this slight upregulation under B-deficient growth condition may reflect a physiologically relevant involvement in the adaptation to B deficiency remains to be demonstrated. Moreover, we observed that in the natural accessions, differences in the expression level of *HvNIP2;2/HvLsi6* and its fold-change were significantly correlated with root dry weight (Figure 5C,D). During seed development, it was found that the expression level of *HvNIP2;2/HvLsi6* before grain filling is more than a 100-fold higher than that in the filled grains (Figure 4I), proposing that a high expression of *HvNIP2;2/HvLsi6* is a prerequisite for B provision to grains. Our results show that *HvNIP2;2/HvLsi6* is likely involved in B distribution and transport besides its previously described role in determining Si distribution (Yamaji et al., 2012). This qualifies *HvNIP2;2/HvLsi6* as a transport protein contributing to the maintenance of the overall metalloid nutritional status in barley. However, the absence of *HvNIP2;2/HvLsi6* in endosperm transfer cells of barley grains (Thiel, 2014) and our expression analysis revealed that it is not involved in the very last step

of grain B loading. The molecular mechanism of this final transport process remains to be identified.

ACKNOWLEDGMENTS

The authors acknowledge Dr. Yudelys Tandron Moya for excellent technical assistance in the ICP-OES and ICP-MS analysis, Jacqueline Fuge for RT-qPCR analysis and plasmid construction, and Kristin Vorpahl for plasmid construction and cloning (all IPK, Gatersleben). The authors thank Dr. Benjamin D. Gruber for conducting and taking care of field trials. The authors also thank Dr. Benjamin Kilian for sharing seeds of natural accessions for the GWAS panel. The authors finally acknowledge the funding by the Bundesministerium für Bildung und Forschung, Germany, in frame of the “BARSELECT” project granted to N.v.W. (FKZ0315969D), by a scholarship of the Chinese Scholarship Council (CSC) to Z.T.J. (No. 201406350062), and by an Emmy Noether grant from the Deutsche Forschungsgemeinschaft (DFG) to G.P.B. (1668/1-1). Moreover, this project was carried out in part in the framework of the priority program 2089 “Rhizosphere spatiotemporal organization—a key to rhizosphere functions” funded by the DFG (1668/4-1). Open access funding enabled and organized by Projekt DEAL.

AUTHOR CONTRIBUTIONS

Zhongtao Jia performed most experiments and GWAS. Manuela D. Bienert conducted yeast growth assay, performed gene cloning and plasmid construction, and designed RT-qPCR primers. Gerd P. Bienert performed B uptake assay in *X. laevis* oocytes. Zhongtao Jia, Manuela D. Bienert, Nicolaus von Wirén, and Gerd P. Bienert designed experiments, analyzed the data, and wrote the manuscript. All authors read and approved the final manuscript.


DATA AVAILABILITY STATEMENT

Data supporting the findings of this study are available within the manuscript and its Supporting Information files. Datasets generated and analyzed during the current study are available from the corresponding author on reasonable request.

ORCID

Zhongtao Jia  <https://orcid.org/0000-0003-0233-1578>

Manuela Désirée Bienert  <https://orcid.org/0000-0001-5948-3789>

Nicolaus von Wirén  <https://orcid.org/0000-0002-4966-425X>

Gerd Patrick Bienert  <https://orcid.org/0000-0001-9345-4666>

REFERENCES

- Abdel-Ghani, A.H., Sharma, R., Wabila, C., Dhanagond, S., Owais, S.J., Duwayri, M.A., et al. (2019) Genome-wide association mapping in a diverse spring barley collection reveals the presence of QTL hotspots and candidate genes for root and shoot architecture traits at seedling stage. *BMC Plant Biology*, 19(216).
- Alamri, S.A., Siddiqui, M.H., Al-Khaisani, M.Y. & Ali, H.M. (2018) Boron induces seed germination and seedling growth of *Hordeum vulgare* L. under NaCl stress. *Journal of Advance Agricultural Research*, 8, 1224–1234.
- Alqudah, A.M., Sharma, R., Pasam, R.K., Graner, A., Kilian, B., & Schnurbusch, T. (2014) Genetic dissection of photoperiod response

- based on GWAS of pre-anthesis phase duration in spring barley. *PLoS One*, 9(e113120).
- Alqudah, A.M., Koppolu, R., Wolde, G.M., Graner, A. & Schnurbusch, T. (2016) The genetic architecture of barley plant stature. *Frontiers in Genetics*, 7(117).
- Alqudah, A.M., Youssef, H.M., Graner, A. & Schnurbusch, T. (2018) Natural variation and genetic make-up of leaf blade area in spring barley. *Theoretical and Applied Genetics*, 131, 873–886.
- Atique-ur-Rehman, F.M., Cheema, Z.A. & Wahid, A. (2012) Seed priming with boron improves growth and yield of fine grain aromatic rice. *Plant Growth Regulation*, 68, 189–201.
- Bienert, G.P., Bienert, M.D., Jahn, T.P., Boutry, M. & Chaumont, F. (2011) Solanaceae XIPs are plasma membrane aquaporins that facilitate the transport of many uncharged substrates. *The Plant Journal*, 66, 306–317.
- Bienert, M.D. & Bienert, G.P. (2017) Plant aquaporins and metalloids. In: Chaumont, F. & Tyerman, S. (Eds.) *Plant aquaporins. Signaling and communication in plants*. Cham: Springer International, pp. 297–332.
- Bienert, M.D., Muries, B., Crappe, D., Chaumont, F. & Bienert, G.P. (2019) Overexpression of X intrinsic protein 1;1 in *Nicotiana tabacum* and *Arabidopsis* reduces boron allocation to shoot sink tissues. *Plant Direct*, 3, e00143.
- Bradbury, P.J., Zhiwu, Z., Kroon, D.E., Casstevens, T.M., Ramdoss, Y. & Buckler, E.S. (2007) TASSEL: software for association mapping of complex traits in diverse samples. *Bioinformatics*, 23, 2633–2635.
- Brdar-Jokanovic, M. (2020) Boron toxicity and deficiency in agricultural plants. *International Journal of Molecular Sciences*, 21, 1424.
- Chatterjee, M., Tabi, Z., Galli, M., Malcomber, S., Buck, A., Muszynski, M., et al. (2014) The boron efflux transporter *ROTTEN EARs* required for maize inflorescence development and fertility. *Plant Cell*, 26, 2962–2977.
- Chiba, Y., Mitani, N., Yamaji, N. & Ma, J.F. (2009) HvLsi1 is a silicon influx transporter in barley. *The Plant Journal*, 57, 810–818.
- Comadran, J., Kilian, B., Russell, J., Ramsay, L., Stein, N., Ganal, M., et al. (2012) Natural variation in a homolog of *Antirrhinum CENTRORADIALIS* contributed to spring growth habit and environmental adaptation in cultivated barley. *Nature Genetics*, 44, 1388–1392.
- Core Team, R. (2013) *R: a language and environment for statistical computing*. Vienna: The R Foundation for Statistical Computing.
- Dell, B. & Huang, L.B. (1997) Physiological response of plants to low boron. *Plant and Soil*, 193, 103–120.
- Di Giorgio, J.P., Bienert, G.P., Ayub, N., Yaneff, A., Barberini, M.L., Mecchia, M.A., et al. (2016) Pollen-specific aquaporins NIP4;1 and NIP4;2 are required for pollen development and pollination in *Arabidopsis thaliana*. *Plant Cell*, 28, 1053–1077.
- Diehn, T.A., Bienert, M.D., Pommerrenig, B., Liu, Z.J., Spitzer, C., Bernhardt, N., et al. (2019) Boron demanding tissues of *Brassica napus* express specific sets of functional Nodulin26-like intrinsic proteins and BOR1 transporters. *The Plant Journal*, 100, 68–82.
- Dordas, C., Chrispeels, M.J. & Brown, P.H. (2000) Permeability and channel-mediated transport of boric acid across membrane vesicles isolated from squash roots. *Plant Physiology*, 124, 1349–1362.
- Durbak, A.R., Phillips, K.A., Pike, S., O'Neill, M., Mares, J., Gallavotti, A., et al. (2014) Transport of boron by the *tassel-less1* aquaporin is critical for vegetative and reproductive development in maize. *Plant Cell*, 26, 2978–2995.
- Eggert, K. & von Wirén, N. (2013) Dynamics and partitioning of the ionome in seeds and germinating seedlings of winter oilseed rape. *Metallomics*, 5, 1316–1325.
- Eggert, K. & von Wirén, N. (2016) The role of boron nutrition in seed vigour of oilseed rape (*Brassica napus* L.). *Plant and Soil*, 402, 63–76.
- Eggert, K. & von Wirén, N. (2017) Response of the plant hormone network to boron deficiency. *The New Phytologist*, 216, 868–881.
- Fitzpatrick, K.L. & Reid, R.J. (2009) The involvement of aquaglyceroporins in transport of boron in barley roots. *Plant, Cell and Environment*, 32, 1357–1365.
- Hanaoka, H., Uruguchi, S., Takano, J., Tanaka, M. & Fujiwara, T. (2014) OsNIP3;1, a rice boric acid channel, regulates boron distribution and is essential for growth under boron-deficient conditions. *The Plant Journal*, 78, 890–902.
- Hanikenne, M., Talke, I.N., Haydon, M.J., Lanz, C., Nolte, A., Motte, P., et al. (2008) Evolution of metal hyperaccumulation required cis-regulatory changes and triplication of *HMA4*. *Nature*, 453, 391–395.
- Haseneyer, G., Stracke, S., Paul, C., Einfeldt, C., Broda, A., Piepho, H.P., et al. (2010) Population structure and phenotypic variation of a spring barley world collection set up for association studies. *Plant Breed*, 129, 271–279.
- Hua, Y., Zhang, D., Zhou, T., He, M., Ding, G., Shi, L., et al. (2016) Transcriptomics-assisted quantitative trait locus fine mapping for the rapid identification of a nodulin 26-like intrinsic protein gene regulating boron efficiency in allotetraploid rapeseed. *Plant, Cell and Environment*, 39, 1601–1618.
- International Barley Genome Sequencing Consortium, Mayer, K.F., Waugh, R., Brown, J.W.S., Schulman, A., Langridge, P., et al. (2012) A physical, genetic and functional sequence assembly of the barley genome. *Nature*, 491, 711–716.
- Iqbal, S., Farooq, M., Cheema, S.A. & Afzal, I. (2017) Boron seed priming improves the seedling emergence, growth, grain yield and grain bio-fortification of bread wheat. *International Journal of Agriculture and Biology*, 19, 177–182.
- Jamjod, S., Nirunrayagul, S. & Rerkasem, B. (2004) Genetic control of boron efficiency in wheat (*Triticum aestivum* L.). *Euphytica*, 135, 21–27.
- Jia, Z.T., Giehl, R.F.H., Meyer, R.C., Altmann, T. & von Wirén, N. (2019) Natural variation of BSK3 tunes brassinosteroid signaling to regulate root foraging under low nitrogen. *Nature Communications*, 10, 2378.
- Jia, Z.T., Giehl, R.F.H. & von Wirén, N. (2020) The root foraging response under low nitrogen depends on DWARF1-mediated brassinosteroid biosynthesis. *Plant Physiology*, 183, 998–1010.
- Jia, Z.T., Liu, Y., Gruber, B.D., Neumann, K., Kilian, B., Graner, A., et al. (2019) Genetic dissection of root system architectural traits in spring barley. *Frontiers in Plant Science*, 10, 400.
- Kuhlmann, M., Meyer, R.C., Jia, Z., Klose, D., Krieg, L.M., von Wirén, N., et al. (2020) Epigenetic variation at a genomic locus affecting biomass accumulation under low nitrogen in *Arabidopsis thaliana*. *Agronomy*, 10, 636.
- Kumar, K., Mosa, K.A., Chhikara, S., Musante, C., White, J.C. & Dhankher, O.P. (2014) Two rice plasma membrane intrinsic proteins, OsPIP2;4 and OsPIP2;7, are involved in transport and providing tolerance to boron toxicity. *Planta*, 239, 187–198.
- Leonard, A., Holloway, B., Guo, M., Rupe, M., Yu, G.X., Beatty, M., et al. (2014) *tassel-less1* encodes a boron channel protein required for inflorescence development in maize. *Plant and Cell Physiology*, 55, 1044–1054.
- Lewis, D.H. (2019) Boron: the essential element for vascular plants that never was. *The New Phytologist*, 221, 1685–1690.
- Li, T., Choi, W.G., Wallace, I.S., Baudry, J. & Roberts, D.M. (2011) *Arabidopsis thaliana* NIP7;1: an anther-specific boric acid transporter of the aquaporin superfamily regulated by an unusual tyrosine in helix 2 of the transport pore. *Biochemistry*, 50, 6633–6641.
- Liu, J., Yang, J.P., Li, R.Y., Shi, L., Zhang, C.Y., Long, Y., et al. (2009) Analysis of genetic factors that control shoot mineral concentrations in rapeseed (*Brassica napus*) in different boron environments. *Plant and Soil*, 320, 255–266.
- Long, N.V., Dolstra, O., Malosetti, M., Kilian, B., Graner, A., Visser, R.G.F., et al. (2013) Association mapping of salt tolerance in barley (*Hordeum vulgare* L.). *Theoretical and Applied Genetics*, 126, 2335–2351.
- Lordkaew, S., Dell, B., Jamjod, S. & Rerkasem, B. (2011) Boron deficiency in maize. *Plant and Soil*, 342, 207–220.
- Lordkaew, S., Konsaeng, S., Jongjaidee, J., Dell, B., Rerkasem, B. & Jamjod, S. (2013) Variation in responses to boron in rice. *Plant and Soil*, 363, 287–295.
- Ma, J.F., Tamai, K., Yamaji, N., Mitani, N., Konishi, S., Katsuhara, M., et al. (2006) A silicon transporter in rice. *Nature*, 440, 688–691.
- Mascher, M.M., Muehlbauer, G.J., Rokhsar, D.S., Chapman, J., Schmutz, J., Barry, K., et al. (2013) Anchoring and ordering NGS contig assemblies by population sequencing (POPSEQ). *The Plant Journal*, 76, 718–727.

- Matoh, T. (1997) Boron in plant cell walls. *Plant and Soil*, 193, 59–70.
- Matoh, T., Ishigaki, K., Ohno, K. & Azuma, J. (1993) Isolation and characterization of a boron-polysaccharide complex from radish roots. *Plant and Cell Physiology*, 34, 639–642.
- Maurel, C., Boursiac, Y., Luu, D.T., Santoni, V., Shahzad, Z. & Verdoucq, L. (2015) Aquaporins in plants. *Physiological Reviews*, 95, 1321–1358.
- Meacham, S.L., Taper, L.J. & Volpe, S.L. (1995) Effect of boron supplementation on blood and urinary calcium, magnesium, and phosphorus, and urinary boron in athletic and sedentary women. *The American Journal of Clinical Nutrition*, 61, 341–345.
- Mitani-Ueno, N., Yamaji, N., Zhao, F.J. & Ma, J.F. (2011) The aromatic/arginine selectivity filter of NIP aquaporins plays a critical role in substrate selectivity for silicon, boron, and arsenic. *Journal of Experimental Botany*, 62, 4391–4398.
- Miwa, K., Takano, J., Omori, H., Seki, M., Shinozaki, K. & Fujiwara, T. (2007) Plants tolerant of high boron levels. *Science*, 318, 1417.
- Nakagawa, Y., Hanaoka, H., Kobayashi, M., Miyoshi, K., Miwa, K. & Fujiwara, T. (2007) Cell-type specificity of the expression of osBOR1, a rice efflux boron transporter gene, is regulated in response to boron availability for efficient boron uptake and xylem loading. *Plant Cell*, 19, 2624–2635.
- Neumann, K., Zhao, Y.S., Chu, J.T., Keilwagen, J., Reif, J.C., Kilian, B., et al. (2017) Genetic architecture and temporal patterns of biomass accumulation in spring barley revealed by image analysis. *BMC Plant Biology*, 17(137).
- Nielsen, F.H., Hunt, C.D., Mullen, L.M. & Hunt, J.R. (1987) Effect of dietary boron on mineral, estrogen, and testosterone-metabolism in postmenopausal women. *The FASEB Journal*, 1, 394–397.
- Nour-Eldin, H.H., Hansen, B.G., Norholm, M.H., Jensen, J.K. & Halkier, B.A. (2006) Advancing uracil-excision based cloning towards an ideal technique for cloning PCR fragments. *Nucleic Acids Research*, 34, e122.
- Ochiai, K., Uemura, S., Shimizu, A., Okumoto, Y. & Matoh, T. (2008) Boron toxicity in rice (*Oryza sativa* L.). I. Quantitative trait locus (QTL) analysis of tolerance to boron toxicity. *Theoretical and Applied Genetics*, 117, 125–133.
- O'Neill, M.A., Eberhard, S., Albersheim, P. & Darvill, A.G. (2001) Requirement of borate cross-linking of cell wall rhamnogalacturonan II for Arabidopsis growth. *Science*, 294, 846–849.
- Pang, Y.Q., Li, L.J., Ren, F., Lu, P.L., Wei, P.C., Cai, J.H., et al. (2010) Overexpression of the tonoplast aquaporin AtTIP5;1 conferred tolerance to boron toxicity in Arabidopsis. *Journal of Genetics and Genomics*, 37, 389–U352.
- Pasam, R.K., Sharma, R., Malosetti, M., van Eeuwijk, F.A., Haseneyer, G., Kilian, B., et al. (2012) Genome-wide association studies for agronomical traits in a world wide spring barley collection. *BMC Plant Biology*, 12(16).
- Pommerrenig, B., Diehn, T.A. & Bienert, G.P. (2015) Metalloido-porins: essentiality of nodulin 26-like intrinsic proteins in metalloid transport. *Plant Science*, 238, 212–227.
- Pommerrenig, B., Eggert, K. & Bienert, G.P. (2019) Boron deficiency effects on sugar, ionome, and phytohormone profiles of vascular and non-vascular leaf tissues of common plantain (*Plantago major* L.). *International Journal of Molecular Sciences*, 20, 3882.
- Pommerrenig, B., Diehn, T.A., Bernhardt, N., Bienert, M.D., Mitani-Ueno, N., Fuge, J., et al. (2020) Functional evolution of nodulin 26-like intrinsic proteins: from bacterial arsenic detoxification to plant nutrient transport. *New Phytologist*, 225, 1383–1396.
- Reid, R. (2014) Understanding the boron transport network in plants. *Plant and Soil*, 385, 1–13.
- Schnurbusch, T., Hayes, J., Hrmova, M., Baumann, U., Ramesh, S.A., Tyerman, S.D., et al. (2010) Boron toxicity tolerance in barley through reduced expression of the multifunctional aquaporin HvNIP2;1. *Plant Physiology*, 153, 1706–1715.
- Shao, J.F., Yamaji, N., Liu, X.W., Yokosho, K., Shen, R.F. & Ma, J.F. (2018) Preferential distribution of boron to developing tissues is mediated by the intrinsic protein OsNIP3. *Plant Physiology*, 176, 1739–1750.
- Shorrocks, V.M. (1997) The occurrence and correction of boron deficiency. *Plant and Soil*, 193, 121–148.
- Sutton, T., Baumann, U., Hayes, J., Collins, N.C., Shi, B.J., Schnurbusch, T., et al. (2007) Boron-toxicity tolerance in barley arising from efflux transporter amplification. *Science*, 318, 1446–1449.
- Takano, J., Miwa, K. & Fujiwara, T. (2008) Boron transport mechanisms: collaboration of channels and transporters. *Trends in Plant Science*, 13, 451–457.
- Takano, J., Noguchi, K., Yasumori, M., Kobayashi, M., Gajdos, Z., Miwa, K., et al. (2002) Arabidopsis boron transporter for xylem loading. *Nature*, 420, 337–340.
- Takano, J., Tanaka, M., Toyoda, A., Miwa, K., Kasai, K., Fuji, K., et al. (2010) Polar localization and degradation of Arabidopsis boron transporters through distinct trafficking pathways. *Proceedings of the National Academy of Sciences of the United States of America*, 107, 5220–5225.
- Takano, J., Wada, M., Ludewig, U., Schaaf, G., von Wirén, N. & Fujiwara, T. (2006) The Arabidopsis major intrinsic protein NIP5;1 is essential for efficient boron uptake and plant development under boron limitation. *Plant Cell*, 18, 1498–1509.
- Tanaka, M., Wallace, I.S., Takano, J., Roberts, D.M. & Fujiwara, T. (2008) NIP6;1 is a boric acid channel for preferential transport of boron to growing shoot tissues in Arabidopsis. *Plant Cell*, 20, 2860–2875.
- Thiel, J. (2014) Development of endosperm transfer cells in barley. *Frontiers in Plant Science*, 5, 108.
- Wang, C.C., Tang, Z., Zhuang, J.Y., Tang, Z., Huang, X.Y. & Zhao, F.J. (2020) Genetic mapping of ionic quantitative trait loci in rice grain and straw reveals OsMOT1;1 as the putative causal gene for a molybdenum QTL qMo8. *Molecular Genetics and Genomics*, 295, 391–407.
- Wang, W., Ding, G., White, P.J., Wang, M., Zou, J., Xu, F., et al. (2020) Genetic dissection of the shoot and root ionomes of *Brassica napus* grown with contrasting phosphate supplies. *Annals of Botany*, 126, 119–140.
- Wimmer, M.A., Abreu, I., Bell, R.W., Bienert, M.D., Brown, P.H., Dell, B., et al. (2020) Boron: an essential element for vascular plants. A comment on Lewis (2019) 'Boron: the essential element for vascular plants that never was'. *New Phytologist*, 226, 1232–1237.
- Wongmo, J., Jamjod, S. & Rerkasem, B. (2004) Contrasting responses to boron deficiency in barley and wheat. *Plant and Soil*, 259, 103–110.
- Yamaji, N., Chiba, Y., Mitani-Ueno, N. & Feng Ma, J. (2012) Functional characterization of a silicon transporter gene implicated in silicon distribution in barley. *Plant Physiology*, 16, 1491–1497.
- Yang, M., Lu, K., Zhao, F.J., Xie, W.B., Ramakrishna, P., Wang, G.Y., et al. (2018) Genome-wide association studies reveal the genetic basis of ionic variation in rice. *Plant Cell*, 30, 2720–2740.
- Zhang, D., Hua, Y., Wang, X., Zhao, H., Shi, L. & Xu, F. (2014) A high-density genetic map identifies a novel major QTL for boron efficiency in oilseed rape (*Brassica napus* L.). *PLoS One*, 9, e112089.
- Zhang, Q., Chen, H.F., He, M.L., Zhao, Z.Q., Cai, H.M., Ding, G.D., et al. (2017) The boron transporter BnaC4.BOR1;1c is critical for inflorescence development and fertility under boron limitation in *Brassica napus*. *Plant, Cell and Environment*, 40, 1819–1833.

SUPPORTING INFORMATION

Additional supporting information may be found online in the Supporting Information section at the end of this article.

How to cite this article: Jia Z, Bienert MD, von Wirén N, Bienert GP. Genome-wide association mapping identifies HvNIP2;2/HvLsi6 accounting for efficient boron transport in barley. *Physiologia Plantarum*. 2021;171:809–822. <https://doi.org/10.1111/ppl.13340>